[CANCER RESEARCH 64, 8613–8619, December 1, 2004]

Coagulation Facilitates Tumor Cell Spreading in the Pulmonary Vasculature during Early Metastatic Colony Formation

Jae Hong Im,[1] Weili Fu,[1] Hui Wang,[1] Sujata K. Bhatia,[3] Daniel A. Hammer,[3] M. Anna Kowalska,[2] and Ruth J. Muschel[1]

Departments of [1]Pathology and [2]Hematology, Children's Hospital of Philadelphia, Philadelphia, Pennsylvania; and [3]Department of Bioengineering and Institute for Medicine and Engineering, University of Pennsylvania, Philadelphia, Pennsylvania

ABSTRACT

Coagulation has long been known to facilitate metastasis. To pinpoint the steps where coagulation might play a role in the metastasis, we used three-dimensional visualization of direct infusion of fluorescence labeled antibody to observe the interaction of tumor cells with platelets and fibrinogen in isolated lung preparations. Tumor cells arrested in the pulmonary vasculature were associated with a clot composed of both platelets and fibrin(ogen). Initially, the cells attached to the pulmonary vessels were rounded. Over the next 2 to 6 hours, they spread on the vessel surface. The associated clot was lysed coincident with tumor cell spreading. To assess the importance of clot formation, we inhibited coagulation with hirudin, a potent inhibitor of thrombin. The number of tumor cells initially arrested in the lung of hirudin-treated mice was essentially the same as in control mice. However, tumor cell spreading and subsequent retention of the tumor cells in the lung was markedly inhibited in the anticoagulated mice. These associations of the tumor cells with platelets were independent of tumor cell expression of P-selectin ligands. This work identifies tumor cell spreading onto the vascular surface as an important component of the metastatic cascade and implicates coagulation in this process.

INTRODUCTION

Metastasis remains the major cause of cancer treatment failure. Tumor dissemination is initiated after the release of tumor cells from the primary tumor into the circulation. Passing through the blood stream, circulating tumor cells eventually produce colonies at remote sites (1). Details of the events required for colonization at distant sites are only superficially understood, but it has been apparent for many years that the coagulation system augments metastasis (2). Since 1968, when Gasic *et al.* (3) showed that experimental pulmonary metastasis is reduced by platelet depletion and restored by supplementation of platelets, there has been much research supporting the concept of enhancement of cancer metastasis by platelets (4). Inhibition of platelet function using integrin subunit α_{IIb} inhibitors or to a lesser effect using aspirin also inhibits metastasis (5, 6). Platelet depletion or anticoagulation only has an inhibitory effect during a short time (0–6 hours) after introduction of the tumor cells into the circulation. Mice without platelets due to genetic elimination of Nf-E2, a transcription factor required in generation of platelets, have greatly reduced ability to support metastasis as do mice deficient in PAR-4 whose platelets are unable to respond to thrombin (7). Deficiency in PAR-1 or PAR-2 thrombin receptors on endothelial cells had no effect on metastasis. Bone metastasis is also enhanced by platelets (8).

Platelets bind to tumor cells *in vivo* and in tissue culture, and this interaction activates platelets leading to their aggregation (9). Morphologic observations show tumor cells closely associated with platelets after vascular arrest (10, 11). A variety of platelet factors contribute to this binding including the glycoproteins, integrin $\alpha_{IIb}\beta_3$ (12–14). P-selectin has also been shown to facilitate metastasis of tumor cells bearing P-selectin ligand (15).

Subsequent work has shown that other components of coagulation also influence metastasis. Inhibition of coagulation by a variety of pharmacologic means reduces pulmonary metastasis (16–18). Fibrinogen has been shown to affect metastasis. Both experimental and spontaneous metastasis are reduced in mice genetically deficient in fibrinogen, but these mice support tumor growth as well as the wild-type mice (19, 20). Some factors involved in coagulation may affect metastasis independently of clot formation by direct action on tumor cells. Plasminogen activator, tissue factor, and tissue factor inhibitors have been shown to contribute independently to the behavior of tumor cells (21–23). Thrombin may have effects not only on clotting, but also on cleavage of the protease-activated thrombin receptor on tumor cells (24–26).

In previous work, we have used observation of isolated lungs at various times after initiation of metastasis to characterize early steps in pulmonary arrest and metastasis (27). Lungs were isolated from rats or mice under physiologic ventilation and perfusion at various times after tumor cells had been injected into the living animal. Such lung preparations are translucent, allowing microscopic observation of the tumor cells and the pulmonary vasculature (28). These studies demonstrated that most of the infused tumor cells initially arrested in the lungs in vessels larger than capillaries. The initial arrest was mediated by the tumor cell integrin $\alpha_3\beta_1$ binding to laminin-5 on basement membrane exposed in the pulmonary blood vessels (29). Extravasation was rare, and the extravasated cells were cleared. As the cells grew, the early colonies were intravascular. These results raised the question of whether platelet interaction with the tumor cells during cellular arrest might affect the arrest or subsequent intravascular colony formation. Accordingly, we developed a method, three-dimensional visualization of direct infusion of fluorescence-labeled antibody (3D-DIFLA), to observe the spontaneous interaction between platelets and tumor cells *in vivo*. Using infusion of fluorescent antibodies against the platelet surface integrin $\alpha_{IIb}\beta_3$, Furie *et al.* (30) were able to observe clot formation after injury in the cremaster muscle. Similarly, we evaluated the extent of platelet binding to various tumor cell lines in isolated lung preparations during colony formation using fluorescent anti-α_{IIb} integrin subunit antibody. Although these antibodies can interfere with platelet function, we avoided this effect by infusing the antibodies after the tumor cells had been introduced, allowing the physiologic interactions to occur.

Consistent with some prior studies, we noted association of the tumor cells with platelets and fibrin or fibrinogen at the time of early arrest. Soon afterward, 6 to 24 hours, we found that as the tumor cells spread onto the vasculature that platelets were no longer seen in aggregates or in association with the tumor cells. Inhibition of coagulation with the thrombin inhibitor hirudin did not alter the initial arrest of the tumor cells, but subsequent spreading and final adhesion was impaired. This work now characterizes pulmonary arrest as

Received 6/11/04; revised 9/10/04; accepted 9/27/04.

Grant support: NIH grants R01 CA89188 and R01 CA46830.

The costs of publication of this article were defrayed in part by the payment of page charges. This article must therefore be hereby marked *advertisement* in accordance with 18 U.S.C. Section 1734 solely to indicate this fact.

Requests for reprints: Ruth J. Muschel, Department of Pathology, Children's Hospital of Philadelphia, Philadelphia, PA, 19104. Phone: 267-426-5481; Fax: 267-426-5483; E-mail: muschel@xrt.upenn.edu.

initially due to contact of the tumor cell with exposed basement followed by spreading of the tumor on the endothelium in a manner morphologically reminiscent of cell spreading in tissue culture. Disruption of clot formation in association with tumor cells prevents this early spreading, but does not appear to directly affect the initial arrest.

MATERIALS AND METHODS

Cell Lines and Culture. The following cell lines were cultured in Dulbecco's modified Eagle's medium (DMEM), 1% streptomycin/penicillin, and 10% heat inactivated fetal bovine serum (FBS): 1205Lu, a human melanoma; B16F10, a mouse melanoma; HT1080, a human fibrosarcoma; and 2.10.10, a rat sarcoma (31–34). LS-180, a human colon adenocarcinoma cell line was cultured in minimal essential medium with 1% streptomycin/penicillin, 10% FBS, 0.1 mmol/L nonessential amino acids, and 1 mmol/L sodium pyruvate (35). WM1789, a human melanoma cell line, was cultured in MCDB 153 medium modified with Leibovitz's L-15 medium, 2% FBS, 5 mg of insulin, and 2 mmol/L $CaCl_2$ (36). All of the cell lines were cultured at 37°C in humidified atmosphere containing 5% CO_2. LS180 and WM1789 were detached with 0.02% EDTA. The other cultured cells were detached using trypsin-EDTA (0.05% trypsin). All the cell lines were transfected with an expression vector for green fluorescent protein (GFP; pEGFP-C1 for 1205Lu and WM1789; pEGFP-C2 for B16F10, 2.10.10 and HT1080; pEGFP-F for LS180; Clontech, Palo Alto, CA). Using flow cytometry, the brightest fluorescent cells (> 95%) were sorted and cloned as in our previous work (27). Stable transfected cells expressing GFP were sustained with medium including G418 sulfate (from 200 to 800 μg/mL depending on the cell line; Cellgro, Herndon, VA). Cells (5×10^6) were plated into 150-cm^2 tissue culture flasks 24 hours before injection and detached in single-cell suspensions as indicated.

Platelet Staining. Platelets were stained with PKH26 using a red fluorescent cell linker kit (Sigma, St. Louis, MO), according to previously reported method (37) and the manufacturer's manual. Immunosuppressed mice (nu/nu, 4–6-week-old females) were purchased from Charles River Laboratories (Horsham, PA). Platelets were washed as described previously (38). In brief, mouse blood was collected from major abdominal vessels with syringes containing ACD buffer [150 μL, 85 mmol/L trisodium citrate, 71 mmol/L citric acid, and 111 mmol dextrose (pH 4.5)]. A washing buffer (3 mL) was added [1 mL of 100 mmol/L EGTA (pH 6.8) and 100 mL of resuspension buffer [2 mL of 7.5% $NaHCO_3$, 133 mL of distilled water, 300 mg of bovine serum albumin, and 15 mL of modified Tyrode's calcium-free buffer; 134 mmol/L NaCl, 3 mmol/L KCl, 0.3 mmol/L $NaH_2PO_4 \cdot H_2O$, 5 mmol/L HEPES, 5 mmol/L glucose, and 2 mmol/L $MgCl_2$ (pH 7.2)]]. The tube was centrifuged at $180 \times g$ and 22°C for 10 minutes. Platelet-rich plasma was collected, and a washing buffer containing prostaglandin E_1 (0.25 μmol/L) was added for total volume of 10 mL. The tube was centrifuged at $1250 \times g$ and 22°C for 10 minutes. Pelleted platelets were washed twice with 10 mL of washing buffer and 0.25 μmol/L prostaglandin E_1. Platelets were counted in a Coulter counter (CDC Technology, Oxford, CT), readjusted to $8 \times 10^5/\mu$L, and stained with PKH26 following the manufacturer's method. The staining reaction was stopped by the addition of 10 mL of citrate-albumin buffer [11 mmol/L glucose, 128 mmol/L NaCl, 4.3 mmol/L NaH_2PO_4 H_2O, 7.5 mmol/L Na_2HPO_4, 4.8 mmol/L sodium citrate, 2.4 mmol/L citric acid, and 0.35% bovine serum albumin (pH 6.5)] with 0.25 μmol/L prostaglandin E_1. Platelets were centrifuged at $1250 \times g$ and 22°C for 20 minutes. Platelets were resuspended at $6 \times 10^6/\mu$L in the resuspension buffer for use. Stained platelets could be kept at room temperature for as long as 24 hours.

Fluorescence-Labeled Antibody to Detect Platelets. Rat antimouse integrin α_{IIb} antibody (IgG1 monoclonal; Santa Cruz Biotechnology, Santa Cruz, CA) was labeled with Alexa Fluor 647 by reaction of fluorescently tagged anti-immunoglobulin G_1 (anti-IgG1) Fc fragment (Zenon-one IgG1 labeling kit; Molecular Probes, Eugene, OR). Excess labeling agent was neutralized by addition of nonspecific IgG. The labeled antibodies were used immediately after preparation.

To test the ability of this tagged antibody to recognize murine platelets, we examined the colocalization of the antibody with PKH26-labeled platelets. B16F10-GFP (1×10^4) were plated into each well of a Chamber Slide (Nalge Nunc International Corp., Napervile, IL) and incubated at 37°C in a humidified atmosphere containing 5% CO_2 for 24 hours. After the removal of the medium, the slide was washed two times with 400 μL of PBS. B16F10 culture medium (200 μL) was added, and PKH26-labeled platelets (5 μL; 3×10^7) were dropped into each well. The slide was incubated at room temperature for 2 hours with gentle shaking in darkness. The Alexa Fluor 647-labeled platelet–specific antimouse integrin α_{IIb} antibody (2 μg) was added and incubated at room temperature for 5 minutes with gentle shaking under darkness. The slide was washed twice with 400 μL of PBS, dried, and analyzed with laser scanning confocal microscopy (Bio-Rad, Hercules, CA).

Three-Dimensional Visualization of Direct Infusion of Fluorescence-Labeled Antibody. An established intact lung microscopy technique (27, 28) was modified and applied to observe tumor cells, platelets, and fibrinogen in the mouse lung. Tumor cells (1×10^6 cells/150 μL in single-cell suspension in DMEM) were injected into a tail vein of each mouse (nu/nu). In those experiments using PKH26-labeled platelets and B16F10-GFP, mice were infused with the labeled platelets immediately after the injection of tumor cells.

At the indicated times, mice were anesthetized, a tracheostomy was introduced, and artificial ventilation was started through a cannula. The abdomen was opened, and Alexa Fluor 647-labeled platelet–specific antibody (10 μg) was infused through the vena cava. For 5-minute time points, the cells were injected through the vena cava, and 5 minutes later, the labeled antibody was also infused. Then after 5 minutes, a mouse was exsanguinated by transection of major abdominal vessels. A cannula was inserted into the main pulmonary artery through a puncture in the right ventricle and another was inserted into the left atrium. The lung was cleared of blood by gravity perfusion through the pulmonary artery with artificial medium [KRB buffer with 5% dextran and 10 mmol/L glucose (pH 7.4)]. The "flow-through" perfusate left the lung through the left atrial cannula. Once the lung became visibly cleared of blood, Alexa Fluor 555-labeled rabbit antimouse fibrinogen antibody (10 μg; Molecular Innovations Inc., Southfield, MI) was infused into the pulmonary artery. The heart–lung preparation was dissected and placed in a specially designed plexiglass chamber with a port to the artificial cannula. The lung rested on a coverslip window at the bottom of the chamber with the posterior surface of the lung touching the coverslip. The lung was ventilated throughout the experiment with 5% CO_2 in medical air and perfused by gravity perfusion except during imaging.

Using laser scanning confocal microscopy, we observed the fluorescently labeled platelets, fibrinogen, and tumor cells in pulmonary vessels and reconstructed their images in three dimensions. The microscopy was performed with Bioradiance 2000 system (Bio-Rad) with Eclipse TE 300 microscope (Nikon, Tokyo, Japan). Laser scanning was simultaneously operated with three light channels: argon (λ_{ex} 488 and 514 nm), helium neon (λ_{ex} 543 nm), and the red laser diode (λ_{ex} 638 nm). Three-dimensional reconstruction of the obtained data was performed by Lasersharp version 4.1 software (Bio-Rad).

P-Selectin Ligand Evaluation. The human P-selectin-IgG chimera was obtained from R&D Systems (Minneapolis, MN). This chimera consists of lectin, epidermal growth factor, and multiple short consensus repeat domains for human P-selectin linked to the Fc region of human IgG. P-Selectin chimera [5 g/mL in PBS (pH 7.4)] was incubated on silanated glass microscope slides of modified flexiPERM wells (Sigma) for at least 2 hours at room temperature with gentle mixing. Slides were then washed with PBS and incubated with blocking buffer (2% heat inactivated bovine serum albumin in PBS) for at least 1 hour at room temperature to prevent nonspecific adhesion.

All experiments were conducted in a parallel plate flow chamber with a tapered channel design based on the Hele-Shaw flow theory between parallel plates (39). The selectin-coated microscope slides served as the bottom plate of the flow chamber. During experiments, the chamber was secured on the stage of a Nikon Diaphot inverted phase contrast microscope connected to a monochrome CCD video camera (Cohu Inc., San Diego, CA) and an S-VHS videocassette recorder (SVO-9500MD; Sony Electronics, Park Ridge, NJ). Buffer and cell suspensions were drawn through the chamber by an infusion/withdrawal syringe pump (Harvard Apparatus, South Natick, MA). Selectin-coated slides were placed in the well of the flow chamber, which was assembled in PBS to prevent air bubbles and then secured on the microscope stage. After perfusion of the chamber with PBS, cells (5×10^5/mL in PBS) were introduced into the flow channel. Data were collected by stepping down the chamber from inlet to outlet in 5-mm steps, allowing at least 1 minute between steps. Cell interaction with the surface was recorded at a total magnification of 300× (using a 10× objective). P-Selectin ligand density on

tumor cell surface was calculated by rolling-velocity comparison of the cells and the beads coated with P-selectin ligand (40).

Determination of Numbers of Arrested Cells. Tumor cells on the pulmonary surface were counted to investigate the effect of platelet clot on tumor cell attachment at early metastasis with recombinant hirudin from yeast cells (Refludan; Berlex Laboratories, Wayne, NJ). Hirudin was reconstituted as directed by the manufacturer and diluted in sterile PBS. Diluted hirudin (100 μL) was injected into a tail vein of each mouse (nu/nu) at a dose of 10 mg/kg. The same volume of sterile PBS was injected into each mouse. Twenty minutes after injection of hirudin or PBS, 1205Lu-GFP, human melanoma cells or B16F10-GFP, and murine melanoma cells (5×10^5 cells/150 μL in single-cell suspension in DMEM) were also injected into a tail vein of the mouse. For 5-minute time points, the cells were injected through the vena cava. Lung was perfused and isolated as previously explained. The pulmonary surface was observed and recorded with an inverted fluorescent microscope (DMIRB; Leica, Wetzlar, Germany), a digital camera (Orca; Hamamatsu Photonics, Hamamatsu, Japan), and Open Lab software (Improvision, Coventry, United Kingdom). Cell numbers were counted in 60 consecutive and nonoverlapping fields with a 20×/1.5× lens (0.122 mm^2 field per picture). All experiments were independently performed at least three times.

Clotting Time. Hirudin effect on anticoagulation was evaluated with the activated partial thromboplastin time (38). The blood was collected from major abdominal vessels just before lung isolation and centrifuged for 10 minutes at $3000 \times g$ at 4°C to obtain plasma. Automated activated partial thromboplastin time reagent (200 μL; BioMerieux, Inc., Durham, NC) was added to 200 μL of plasma. Clotting was initiated by addition of $CaCl_2$ (2 mol/L) 100 μL. Time for clotting was measured by a BioMerieux recorder.

RESULTS

Platelet Visualization *In vivo*. We used an antimouse α_{IIb} integrin subunit monoclonal antibody to visualize platelets, because platelets specifically express the integrin $\alpha_{IIb}\beta_3$. To test the use of this antibody to visualize platelets, we labeled platelets with PKH26 and then asked whether the antibody allowed microscopic detection of these labeled platelets. PKH26 labeling does not activate platelets, nor does it affect platelet response to thrombin or ADP (41). PKH26-labeled platelets were incubated with mouse melanoma cells B16F10-GFP in tissue culture resulting in aggregates of platelets surrounding the tumor cells. The antimouse α_{IIb} integrin subunit antibody fluorescently labeled by coupling to an anti-IgG1 Fc tagged with Alexa Fluor 647 was then added to the culture. Signal from the PHK26 (red) colocalized with the fluorescent antibody (blue). Characteristic images are shown in Fig. 1*A* through *D*. PGE 1 was used as a platelet aggregation inhibitor during the preparation of the platelets, but was omitted from the incubation to eliminate any possible effect of prostaglandin E_1 on the cells. The images clearly showed that the antibody reacted with the platelets on the tumor cell surface.

To validate the use of this antibody *in vivo*, we infused B16F10-GFP cells intravenously followed by infusion of PHK26-labeled platelets. Two hours later, the Alexa Fluor 647-labeled anti-α_{IIb} integrin subunit antibody was infused into the vena cava followed by isolation of the lung. The free antibody was washed out by the perfusion of the pulmonary vessels during the lung preparation. In the isolated lung, PKH26-labeled platelets were seen surrounding tumor cells (Fig. 1*H*). The antibody colocalized with the PKH26-labeled platelets. There was additional staining with the antibody beyond the PHK26 signal, which we attribute to reaction of the antibody with endogenous platelets that were not labeled with PKH26 (Fig. 1*F* and *G*). These experiments verified that platelets could be detected in pulmonary vessels in isolated lungs using antimouse α_{IIb} integrin subunit antibody, and that this would be a suitable methodology to use to examine the association of platelets with tumor cells during arrest in the pulmonary vasculature.

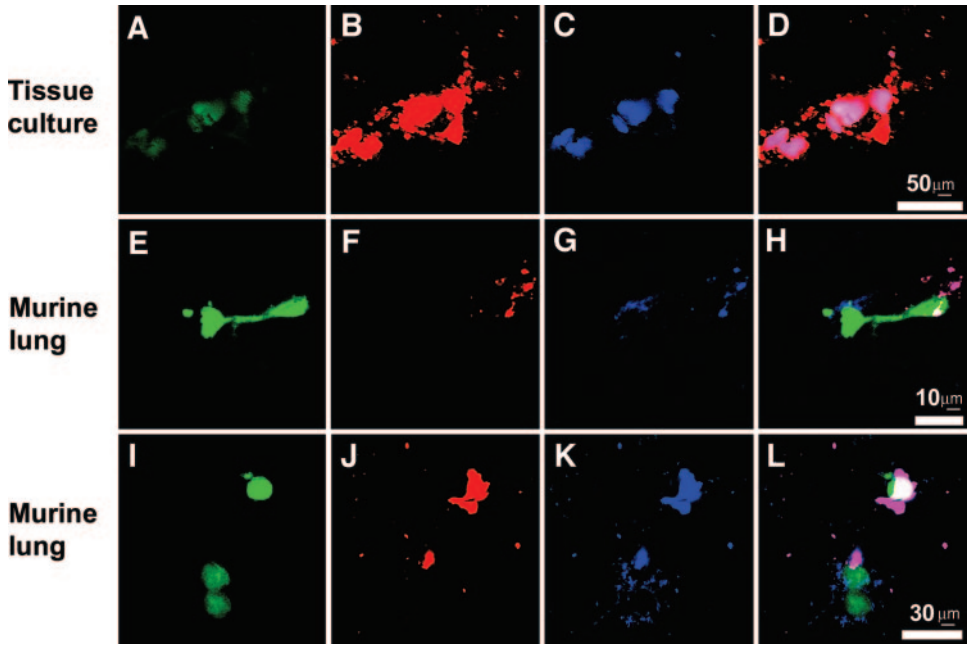

Fig. 1. Antibodies recognize the α_{IIb} integrin of platelets *in vitro* and *in vivo*, and fibrinogen *in vivo*. *A* through *H*. Platelets were labeled with the fluorescent dye PHK26 (*red*), and the antimouse α_{IIb} integrin subunit antibody was labeled with an anti-IgG1 Alexa Fluor 647-tagged Fc fragment (*blue*). B16F10-GFP constitutively expresses GFP (*green*). Colocalization of all three colors (*green*, *red*, and *blue*) appears *white*. *A* through *D*. Tumor cells in tissue culture were incubated with the labeled platelets. *A* shows several tumor cells. *B* shows the platelets surrounding the tumor cell. *C* shows the antibody staining of the platelets. *D* is the merged image. *E* through *H*. Platelets are imaged in a murine lung. B16F10-GFP cells were infused into a mouse. Then the PHK-labeled platelets were infused so that approximately 50% of the platelets would be labeled. After 2 hours, the labeled antibody was infused, the lungs were isolated and imaged. *E* shows a tumor cell. *F* shows the PHK platelets surrounding the tumor cell. *G* shows the antibody staining of the platelets and *H* is the merged image. *I* through *L*. Platelets and fibrinogen are imaged in murine lung. 1205Lu-GFP cells (*green*) and Alexa Fluor 647-labeled antimouse α_{IIb} integrin subunit antibody (*blue*) were infused into the vena cava. After clearing of blood from lung by perfusion with artificial medium (KRB buffer), Alexa Fluor 555-labeled fibrinogen-specific antibody (*red*) was infused into the pulmonary artery. The heart–lung preparation was dissected and imaged. *I* shows 1205Lu-GFP cells. *J* shows the antibody staining of fibrinogen surrounding tumor cells. *K* shows the antibody staining of the platelets, and *L* is the merged image.

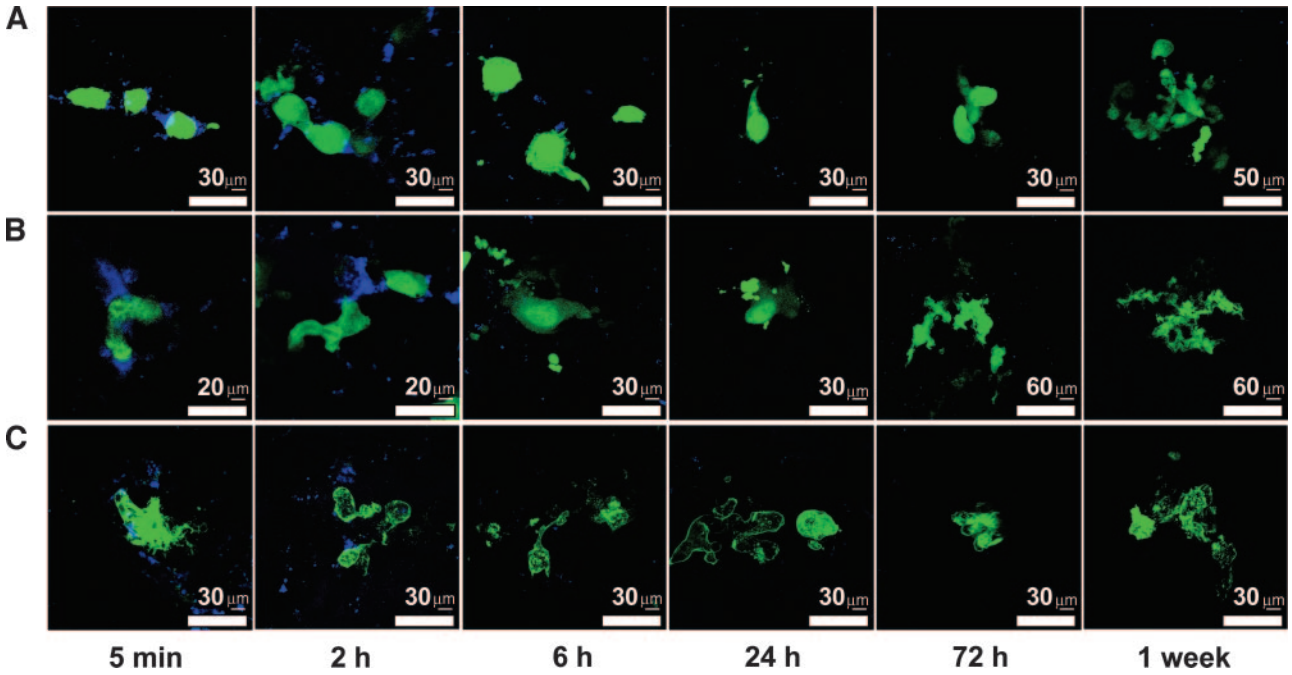

Fig. 2. Time course of platelet association with tumor cells *in vivo*. Tumor cells stably expressing GFP were injected intravenously into mice. After the indicated times, antimouse α_{IIb} integrin subunit antibody tagged with Alexa Fluor 647 was infused, and the lungs were immediately isolated and imaged. The images shown are as viewed from the top-down. *A*, 1205Lu-GFP cells; *B*, B16F10-GFP cells; and *C*, LS180-GFP cells.

Table 1 *Platelet interaction with tumor cell lines in vivo*

Cell lines	Origin	P-selectin ligand	Time 5 min	2 h	6 h	24 h	72 h	1 wk
LS180	Human adenocarcinoma	+	+	+	+	−	−	−
1205Lu	Human melanoma	−	+	+	+	−	−	−
B16F10	Mouse melanoma	−	+	+	+	−	−	−
HT1080	Human fibrosarcoma	−	+	ND	ND	−	ND	ND
WM1789	Human melanoma	−	+	ND	ND	−	ND	ND
2.10.10	Rat sarcoma	−	+	ND	ND	−	ND	ND

Abbreviation: ND, not done.

Association with Fibrin(ogen). To ask whether fibrinogen was incorporated into the platelet aggregates, we infused antibodies against murine fibrinogen labeled with Alexa fluor 555 (red) along with the labeled antiplatelet integrin subunit α_{IIb} antibody. We could detect fibrin or firbinogen colocalized with platelets coalesced around 1205Lu-GFP *in vivo* (Fig. 1*I–L*). It is formally possible that the material detected is fibrinogen that has not polymerized into fibrin. Making this distinction is difficult because murine antibodies that distinguish fibrin from fibrinogen are not available. Nonetheless, the implication is that these platelets are enmeshed fibrin(ogen) as would be expected for a true clot and not for platelet aggregation alone.

Three-Dimensional Visualization of Platelet–Tumor Cell Interactions in Pulmonary Vessels. We examined the association of platelets with tumor cells during the pulmonary arrest of six different cell lines (Table 1). Antimouse α_{IIb} integrin subunit antibody labeled with Alexa Fluor 647 was infused immediately before lung isolation. Five minutes after tumor cell injection, platelets were seen associated with tumor cells. In most cases, the platelets appeared coalesced in the shape of a comet tail emanating from the tumor cell, rather than uniformly coating the surface of the tumor cell (Fig. 2). The time course of tumor cell–platelet interaction was examined in more detail using three cell lines: 1205Lu human melanoma, B16F10 mouse melanoma, and LS180 human colon adenocarcinoma. Eighty percent of 1205Lu-GFP cells were associated with platelets 5 minutes after tumor cell injection, and 60% were associated 2 hours after infusion (Fig. 3). These numbers were similar for all cell lines tested. At 6 or 24 hours, most tumor cells were no longer associated with platelets.

P-Selectin has been shown to influence platelet association with tumor cells and enhance metastasis. The presence of P-selectin ligand on the tumor cell might affect the interaction of tumor cells with platelets. Accordingly, we tested for the presence of P-selectin ligand on the tumor cells we had used. The presence of P-selectin on the tumor cell surface was detected by measuring a decrease in the velocity of tumor cells that bear P-selectin ligands over P-selectin coated surfaces. This method can reliably measure densities of P-selectin ligand as low as 17 molecules (sialy-Lewis^x) per square micrometer (40). This method also has the advantage that it is based on functionality of the P-selectin ligand and does not presuppose the

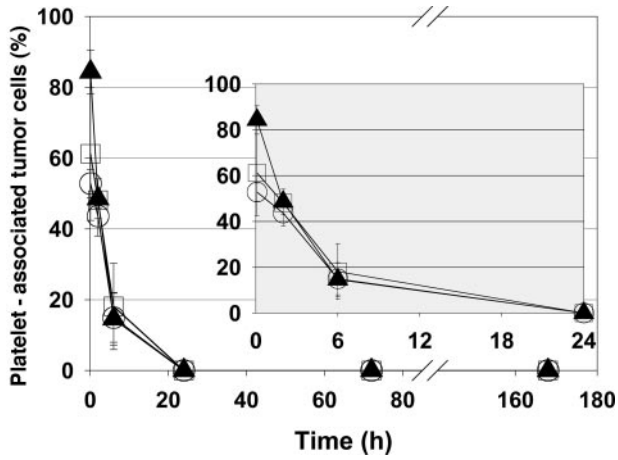

Fig. 3. Tumor cell association with platelets in the lung. Tumor cells 1205Lu-GFP (▲), B16F10-GFP (○), and LS180-GFP (□) were infused into mice (nu/nu). At the indicated times, antimouse α_{IIb} integrin subunit antibody tagged with Alexa Fluor 647 was infused, immediately followed by lung isolation as in Fig. 2. The number of tumor cells with associated platelet fluorescence was counted. Each point represents data from at least three independent experiments.

Table 2 *Activated partial thromboplastin time after injection of hirudin*

	aPTT (s)		
	25 min *	2 h, 20 min *	6 h, 20 min *
PBS	68.5 ± 3.2	78.3 ± 7.8	72.0 ± 12.7
Hirudin	>300	>100 (100, 189, >300, >300) †	54.9 ± 3.0

Abbreviation: aPTT, activated partial thromboplastin time.

* Mice (nu/nu) received 10 mg/kg hirudin intravenously. At the indicated times, mice were sacrificed, and blood was obtained from the vena cava for determination of the aPTT.

† At 2 hours, all mice were anticoagulated, but the extent, as indicated by the aPTT, was highly variable. By 6 hours, the effect of hirudin injection was no longer evident.

chemical nature of the ligand. Of the cell lines we had used, only LS180 (Table 1) had detectable P-selectin ligand consistent with the work of Kim *et al.* (42). Interestingly, we did not observe enhanced or prolonged platelet binding by LS180 compared with cells without P-selectin ligand.

Effect of Anticoagulation by Thrombin Inhibition with Hirudin. Mice were anticoagulated by the injection of hirudin before the injection of 1205Lu-GFP or B16F10-GFP cells. Hirudin inhibited coagulation at 5 minutes and at 2 hours, but by 6 hours, the effect was no longer apparent as expected given the known short half-life of hirudin *in vivo* (Table 2). The level of anticoagulation, although still present at 2 hours, was diminished, and its extent was variable from mouse to mouse. In three-dimensional reconstructions, no platelet-clot or fibrin(ogen) was seen surrounding 1205Lu-GFP cells injected into the anticoagulated mice at 5 minutes, 2 or 6 hours after injection (Fig. 4*A* and *B*). In contrast platelets and fibrin(ogen) surrounded virtually all 1205Lu-GFP cells in the control mice at 5 minutes and 2 hours after injection. At 6 hours in the controls, few platelets were apparent adjacent to tumor cells, although fibrin(ogen) still remained (Fig. 4*C* and *D*, *red*). This result is consistent with the data in Fig. 3 that showed the decrement of tumor cells associated with platelets from 80% to about 20% at that time.

We then asked whether the initial pulmonary arrest was affected by anticoagulation (Fig. 4*E*). When hirudin was injected, the numbers of 1205Lu-GFP cells arrested were slightly less than those in the control (93%) at 5 minutes. This difference became more extensive with time; 37 and 26% of the control at 2 and 6 hours, respectively. Similar results were obtained using B16F10-GFP cells.

Morphologic differences between the tumor cells in the hirudin-treated and in the control mice became apparent with time. When lungs were examined at 5 minutes after the injection of tumor cells,

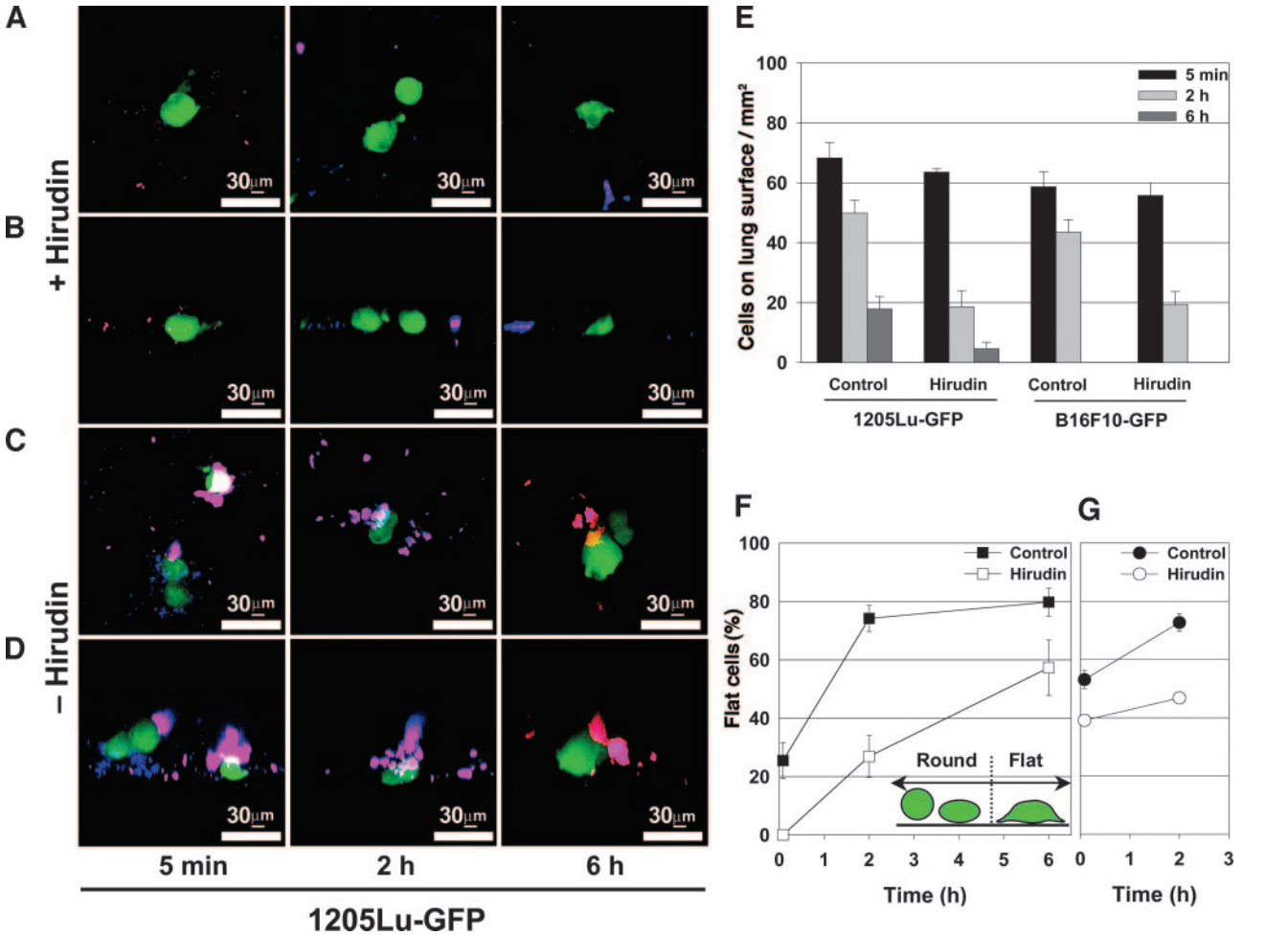

Fig. 4. Hirudin effect on tumor cell behavior on murine pulmonary surface. Twenty minutes after injection of diluted hirudin or PBS, 1205Lu-GFP or B16F10-GFP (*green*, 0.5×10^6 cells) were also injected intravenously into mice. After the indicated times, Alexa Fluor 647-labeled antimouse α_{IIb} integrin (*blue*) subunit antibody and Alexa Fluor 555-labeled fibrinogen–specific antibody (*red*) were infused. *A* through *D*, three-dimensional reconstructed images obtained from laser scanning confocal microscopy of 1205Lu-GFP cells. *A* (*top view*) and *B* (*lateral view*) were obtained after hirudin was injected, whereas *C* (*top view*) and *D* (*lateral view*) were obtained when PBS was injected. *White* shows colocalization of platelets (*blue*) and fibrin(ogen) (*red*) surrounding 1205Lu-GFP (*green*). In *E*, the pulmonary surface was observed and recorded with an inverted fluorescent microscope. Cell numbers were counted in 60 consecutive and nonoverlapping fields with a 20×/1.5× lens (0.122 mm^2 field per picture). *F* (1205Lu-GFP) and *G* (B16F10-GFP) show the quantification of cell morphologic change. Three-dimensional reconstructed images of tumor cells were scored as round and flat on the basis of shapes shown in *green*. Each point represents data from at least three independent experiments.

most tumor cells were rounded and only had limited contacts with the vessel. The tumor cells in control experiments were seen to flatten onto the surface of the vessels as soon as 5 minutes after injection. We measured this difference determining the percentage of flattened cell numbers in three-dimensional reconstructed images (Fig. 4*F* and *G*). To measure the differences in cell shape, we defined a round cell as one with its greatest diameter in the middle rather than at the ends of the cell. A flat cell was identified as one with its greatest diameter adjacent to its end or to the vessel surface. Cell shape was evaluated using z series obtained at 0.5-μm intervals across the cell. After three-dimensional reconstruction and rotation, the diameters were compared across the middle and the ends of the cell, and the cells were classified as either round or flat based on these criteria. This distinction was briefly shown at Fig. 4*F*. There were striking differences between 1205Lu-GFP cells in the hirudin-treated mice and the controls. Many fewer cells were spread or flattened in the hirudin-treated mice while the mice were anticoagulated. By 6 hours, when the mice were no longer anticoagulated, the few remaining tumor cells in the mice that had received hirudin had also flattened on the vessel wall. Hirudin had a similar effect on the shape of B16F10-GFP cells. Although a larger number of B16F10 were flat at the earliest times observed, hirudin treatment also limited the spreading of those cells.

DISCUSSION

Inhibition of coagulation has long been known to drastically reduce metastasis. In this study, we have established methods that allow the observation of tumor cells, platelets, and fibrinogen in the pulmonary circulation in isolated lungs. Using these methods, we have detailed the formation of clots during the initial steps in pulmonary arrest. In addition, we have shown that disruption of coagulation leads to failure of tumor cell spreading, and fewer cells retained in the lungs.

We have established a new method: 3D-DIFLA. 3D-DIFLA was validated in tissue culture and *in vivo*: first, showing that antimouse integrin α_{IIb} antibody reacts with platelets bound to cells in tissue culture; and second, showing that the fluorescently labeled antibodies could be used to visualize platelets and fibrin(ogen) in the pulmonary vasculature. This method should be generally applicable to any vascular component and could clearly help other researchers to observe vascular components with antibodies for applications in pulmonary medicine, cell biology, or immunology.

Using 3D-DIFLA, we observed that platelet-fibrin(ogen) clots were formed in proximity to tumor cells within 5 minutes of infusion. A detailed time course showed that the association of tumor cells with platelet-fibrin(ogen) clots drastically decreased between 2 and 6 hours after infusion of the tumor cells. By 24 hours, platelets were no longer detected in association with tumor cells. These expand the observations of Sindelar *et al.* (10) and Crissman *et al.* (11) of tumor cells and platelets in the lungs using electron microscopy. This pattern occurred despite expression of P-selectin and was not related to the use of trypsin for cell detachment. The time dependence of platelet binding to tumor cells correlated with tumor cell spreading on the pulmonary vasculature. As the attached tumor cells spread, platelet binding was decreased. When hirudin was injected before tumor cell infusion to inhibit coagulation, the platelet–fibrin(ogen) clots were not observed from 0 to 2 hours. Morphologic changes of tumor cells were drastically inhibited. The numbers of cells initially arrested were similar to the controls, but the number of cells retained decreased.

Clots have been proposed to function in the metastatic process through a variety of mechanisms including protecting cancer cells from natural killer cells or from the physical stress of blood flow, facilitating tumor cell attachment to vessel walls, contributing proteolytic enzymes that could enhance extravasation, enhancing angiogenesis, or assisting in endothelial cell retraction (6, 43–45). The components of coagulation individually can be shown to affect metastasis. Using fibrinogen-deficient mice, Palumbo *et al.* (20) showed that fibrinogen plays a role in adhesion and survival of tumor cells rather than growth of the tumor cells. The absence of platelets induced either through administration of pharmacologic agents or through the use of mice genetically unable to make platelets leads to reduced metastasis. Inhibition of thrombin diminishes metastasis and mice defective in PAR-4, the platelet thrombin receptors also have reduced metastasis. Thus an intact coagulation system overall seems necessary to facilitate metastasis.

In our earlier work, we had shown that tumor cells tend to arrest in the lung in vessels of larger diameter than capillaries, probably in precapillary arterioles (27). Although arrest in other vascular beds depends on trapping due to size restriction (especially well studied in liver; ref. 46), in the lung, this did not seem to be the predominant factor. Instead, tumor cell $\alpha_3\beta_1$ integrin engages its ligand laminin-5 within the vascular bed. Laminin-5, a predominantly basement membrane molecule is available to the integrin in exposed patches of basement membrane in the pulmonary vasculature. These contact points are evident in electron microscopy (29). These events appear to be independent of coagulation, because the initial tumor cell arrest was only slightly affected by inhibition of coagulation.

Taken together with our earlier work and the published literature, we can now formulate a more detailed model of the early events in tumor cell arrest in the lung. As tumor cells are released from the primary tumor into the circulation, platelet–fibrin(ogen) clots form surrounding tumor cells. These clots may protect tumor cells from immunologic and physiologic stresses in the blood stream. The tumor cell then arrests in the pulmonary vasculature using its integrin $\alpha_3\beta_1$ to bind to the vasculature laminin-5. Honn *et al.* (6) suggested that platelet activation may cause retraction of endothelial cells in the pulmonary vasculature. The increased area of available basement membrane by endothelial cell retraction then may provide a surface for tumor cell spreading.

The *in vivo* spreading of tumor cells within vessels has not been described previously, to our knowledge. However, cells have been shown to incorporate into intratumoral blood vessels (47). In cell culture, spreading is dependent on integrins and their signaling to the actin cytoskeleton. Whether this is the case *in vivo* remains to be determined. In our previous studies, we had noted that early colony growth seemed to be intravascular (27).

In this work, we introduced a new method (3D-DIFLA) for detection of the platelet–tumor cell interaction in the mouse pulmonary vasculature. We anticipate that this method will provide alternative means for making *in vivo* observations. We confirmed that tumor cell interaction with platelet–fibrin(ogen) is short lived with rapid clot dissolution. We found that tumor cell spreading on the vessels was inhibited in anticoagulated mice. This work now defines a new step required for metastasis and indicates that the coagulation cascade is required to achieve tumor cell spreading on vessels *in vivo*.

ACKNOWLEDGMENTS

We thank the Institute for Environmental Medicine for their assistance with microscopy. We thank M. Poncz (Children's Hospital of Philadelphia), S. Brass (University of Pennsylvania), and B. Furie (Harvard, Boston, MA) for advice.

REFERENCES

1. Bogenrieder T, Herlyn M. Axis of evil: molecular mechanisms of cancer metastasis. Oncogene 2003;22:6524–36.

2. Honn KV, Tang DC, Crissman JD. Platelets and cancer metastasis: a casual relationship? Cancer Metastasis Rev 1992;11:325–51.
3. Gasic GJ, Gasic TB, Stewart CC. Antimetastatic effects associated with platelet reduction. Proc Natl Acad Sci USA 1968;61:46–52.
4. Hejna M, Raderer M, Zielinski CC. Inhibition of metastases by anticoagulants. J Natl Cancer Inst (Bethesda) 1999;91:22–36.
5. Amirkhosravi A, Mousa SA, Amaya M, et al. Inhibition of tumor cell-induced platelet aggregation and lung metastasis by the oral GpIIb/IIIa antagonist XV454. Thromb Haemost 2003;90:549–54.
6. Honn KV, Tang DG, Grossi IM, et al. Enhanced endothelial cell retraction mediated by 12(S)-HETE: a proposed mechanism for the role of platelets in tumor cell metastasis. Exp Cell Res 1994;210:1–9.
7. Camerer E, Qazi AA, Duong DN, et al. Platelets, protease-activated receptors and fibrinogen in hematogenous metastasis. Blood 2004;104:397–401.
8. Bakewell SJ, Nestor P, Prasad S, et al. Platelet and osteoclast beta3 integrins are critical for bone metastasis. Proc Natl Acad Sci USA 2003;100:14205–10.
9. Beviglia L, Stewart GJ, Niewiarowski S. Effect of four disintegrins on the adhesive and metastatic properties of B16F10 melanoma cells in a murine model. Oncol Res 1995;7:7–20.
10. Sindelar WF, Tralka TS, Ketcham AS. Electron microscopic observation on formation of pulmonary metastases. J Surg Res 1975;18:137–61.
11. Crissman JD, Hatfield JS, Menter DG, Sloane B, Honn KV. Morphological study of the interaction of intravascular tumor cells with endothelial cells and subendothelial matrix. Cancer Res 1988;48:4065–72.
12. Tímár J, Ladányi A, Peták I, Jeney A, Kopper L. Molecular pathology of tumor metastasis III: target and combinational therapies. Pathol Oncol Res 2003;9:49–72.
13. Orr FW, Wang HH, Lafrenie RM, Scherbarth S, Nance D. Interaction between cancer cells and the endothelium in metastasis. J Pathol 2000;190:310–29.
14. Steinert BW, Tang DG, Grossi IM, Umbarger LA, Honn KV. Studies on the role of platelet eicosanoid metabolism and integrin alpha IIb beta 3 in tumor-cell-induced platelet aggregation. Int J Cancer 1993;54:92–101.
15. Varki NM, Varki A. Heparin inhibition of selectin-mediated interactions during the hematogenous phase of carcinoma metastasis: rationale for clinical studies in humans. Semin Thromb Hemost 2002;28:53–66.
16. Colucci M, Delaini F, de Bellis Vitti G, et al. Warfarin inhibits both procoagulant activity and metastatic capacity of Lewis lung carcinoma cells: role of vitamin K deficiency. Biochem Pharmacol 1983;32:1689–91.
17. Iwakawa A, Gasic TB, Viner AD, Gasic GJ. Promotion of lung tumor colonization in mice by the synthetic thrombin inhibitor (no. 805) and its reversal by leech salivary gland extracts. Clin Exp Metastasis 1986;4:205–20.
18. Esumi N, Fan D, Filder IJ. Inhibition of murine melanoma experimental metastasis by recombinant desulfatohirudin, a highly specific thrombin inhibitor. Cancer Res 1991; 51:4549–56.
19. Palumbo JS, Potter JM, Kaplan LS, et al. Spontaneous hematogenous and lymphatic metastasis, but not primary tumor growth or angiogenesis, is diminished in fibrinogen-deficient mice. Cancer Res 2002;62:6966–72.
20. Palumbo JS, Kombrinck KW, Drew AF, et al. Fibrinogen is an important determinant of the metastatic potential of circulating tumor cells. Blood 2000;96:3302–9.
21. Ossowski L, Aguirre-Ghiso JA. Urokinase receptor and integrin partnership: coordination of signaling for cell adhesion, migration and growth. Curr Opin Cell Biol 2000;12:613–20.
22. Bromberg ME, Konigsberg WH, Madison JF, Pawashe A, Garen A. Tissue factor promotes melanoma metastasis by a pathway independent of blood coagulation. Proc Natl Acad Sci USA 1995;92:8205–9.
23. Amirkhosravi A, Meyer T, Chang JY, et al. Tissue factor pathway inhibitor reduces experimental lung metastasis of B16 melanoma. Thromb Haemost 2002;87:930–6.
24. Nierodzik ML, Chen K, Takeshita K, et al. Protease-activated receptor 1 (PAR-1) is required and rate-limiting for thrombin-enhanced experimental pulmonary metastasis. Blood 1998;92:3694–700.
25. Nierodzik ML, Klepfish A, Karpatkin S. Role of platelets, thrombin, integrin IIb-IIIa, fibronectin and von Willebrand factor on tumor adhesion in vitro and metastasis in vivo. Thromb Haemost 1995;74:282–90.
26. Nierodzik ML, Kajumo F, Karpatkin S. Effect of thrombin treatment of tumor cells on adhesion of tumor cells to platelets in vitro and tumor metastasis in vivo. Cancer Res 1992;52:3267–72.
27. Al-Medhi AB, Tozawa K, Fisher AB, et al. Intravascular origin of metastasis from the proliferation of endothelium attached tumor cells: a new model for metastasis. Nat Med 2000;6:100–2.
28. Al-Mehdi AB, Zhao G, Dodia C, et al. Endothelial NADPH oxidase as the source of oxidants in lungs exposed to ischemia or high K+. Circ Res 1998;83:730–7.
29. Wang H, Fu W, Im JH, et al. Tumor cell alpha3beta1 integrin and vascular laminin-5 mediate pulmonary arrest and metastasis. J Cell Biol 2004;164:935–41.
30. Falati S, Gross P, Merrill-Skoloff G, Furie BC, Furie B. Real-time in vivo imaging of platelets, tissue factor and fibrin during arterial thrombus formation in the mouse. Nat Med 2002;8:1175–80.
31. Aigner A, Fischer D, Merdan T, et al. Delivery of unmodified bioactive ribozymes by an RNA-stabilizing polyethylenimine (LMW-PEI) efficiently down-regulates gene expression. Gene Ther 2002;9:1700–7.
32. Hosaka Y, Higuchi T, Tsumagari M, Ishii H. Inhibition of invasion and experimental metastasis of murine melanoma cells by human soluble thrombomodulin. Cancer Lett 2000;161:231–40.
33. Volpert OV, Lawler J, Bouck NP. A human fibrosarcoma inhibits systemic angiogenesis and the growth of experimental metastasis via thrombospondin-1. Proc Natl Acad Sci USA 1998;95:6343–8.
34. Hua J, Muschel RJ. Inhibition of matrix metalloproteinase 9 expression by a ryibozyme blocks metastasis in a rat sarcoma model system. Cancer Res 1996; 56:5279–84.
35. McCool DJ, Okada Y, Frostner JF, Frostner GG. Roles of calreticulin and calnexin during musin synthesis in LS180 and HT29/A1 human colonic adenocarcinoma cells. Biochem J. 1999;341:593–600.
36. Satyamoorthy K, DeJesus E, Linnenbach AJ, et al. Melanoma cell lines from different stages of progression and their biological and molecular analyses. Melanoma Res 1997;7:S35–42.
37. Michelson AD, Barnard MR, Hechtman HB, et al. In vivo tracking of platelets: circulating degranulated platelets rapidly lose surface P-selectin but continue to circulate and function. Proc Natl Acad Sci USA 1996;93:11877–82.
38. Eslin DE, Zhang C, Samuels KJ, et al. Transgenic mice studies demonstrate a role for platelet factor 4 in thrombosis: dissociation between anticoagulant and antithrombotic effect of heparin. Blood. In press 2004.
39. Usami S, Chen HH, Zhao Y, Chien S, Skalak R. Design and construction of a linear shear stress flow chamber. Ann Biomed Eng 1993;21:77–83.
40. Rodgers SD, Camphausen RT, Hammer DA. Sialyl Lewis^x-mediated, PSGL-1-independent rolling adhesion on P-selectin. Biophys J 2000;79:694–706.
41. Rand ML, Wang H, Mody M, et al. Concurrent measurement of the survival of two populations of rabbit platelets labeled with either two PKH lipophilic dyes or two concentrations of biotin. Cytometry 2002;47:111–7.
42. Kim YJ, Boris L, Varki NM, Varki A. P-selectin deficiency attenuates tumor growth and metastasis. Proc Natl Acad Sci USA 1998;95:9325–30.
43. Nieswandt B, Hafner M, Echtenacher B, Mannel DN. Lysis of tumor cells by natural killer cells in mice is impeded by platelets. Cancer Res 1999;59:1295–300.
44. Amirkhosravi M, Francis JL. Coagulation activation by MC28 fibrosarcoma cells facilitates lung tumor formation. Thromb Haemost 1995;73:59–65.
45. Verheul HM, Jorna AS, Hoekman K, et al. Vascular endothelial growth factor-stimulated endothelial cells promote adhesion and activation of platelets. Blood 2000;96:4216–21.
46. Chambers AF, Groom AC, MacDonald IC. Dissemination and growth of cancer cells in metastatic sites. Nat Rev Cancer 2002;2:563–72.
47. Hendrix MJ, Seftor EA, Hess AR, Seftor RE. Vasculogenic mimicry and tumour-cell plasticity: lessons from melanoma. Nat Rev Cancer 2003;3:411–21.

Coagulation Facilitates Tumor Cell Spreading in the Pulmonary Vasculature during Early Metastatic Colony Formation

Jae Hong Im, Weili Fu, Hui Wang, et al.

Cancer Res 2004;64:8613-8619.